Proc. NIPR Symp. Antarct. Meteorites, **5**, 136–154, 1992

PETROLOGY AND MINERALOGY OF THE YAMATO-86720 CARBONACEOUS CHONDRITE

Yukio IKEDA, Takaaki NOGUCHI and Makoto KIMURA

Department of Earth Sciences, Ibaraki Universiy, 1–1, Bunkyo 2-chome, Mito 310

Abstract: Phyllosilicate clasts in Yamato-86720 consist mainly of dehydrated serpentine (or chlorite) and sodian talc (or saponite) components, which are the most homogeneous in chemical compositions among those in CM chondrites. They were produced from chondrules by intense hydrous alteration, resulting in the homogeneous composition of the phyllosilicates. Metal spherules and troilite grains in original chondrules have also altered to ovoidal phyllosilicate inclusions and unusual carbonate-phyllosilicates inclusions, respectively. The CaO content of the original chondrules was retained within them as the unusual carbonate-phyllosilicate inclusions, which resulted in the low CaO content of the Y-86720 matrix. The matrix is different in composition from the clast phyllosilicates, suggesting that the two were produced in conditions different from each other. Pyrrhotite grains in clasts and matrix have altered probably to ferrihydrite, which have produced Fe-rich halos around the pyrrhotite grains after the agglomeration of Y-86720 and prior to a heating event. The heating event took place in the final stage of the chondrite formation, resulting in dehydration of phyllosilicates and reduction of ferrihydrite to Co-Ni-poor kamacite.

1. Introduction

The Yamato(Y)-86720 chondrite is an unusual carbonaceous chondrite having some characteristics of both CI and CM chondrites. This chondrite is one of the three Antarctic unusual carbonaceous chondrites, Belgica(B)-7904, Y-86720, and Y-82162, studied by a research consortium (Leader: Y. IKEDA), and this study has been carried out as a consortium study.

The three unusual carbonaceous chondrites have whole rock oxygen isotopic compositions similar to each other (MAYEDA and CLAYTON, 1990; MAYEDA *et al.*, 1991). However, the three chondrites are different in mineralogy and petrology to each other; Y-82162 has no chondrules, Y-86720 has some completely altered chondrules, and B-7904 has many partially altered chondrules. No primary olivine occurs in Y-82162, pseudomorphs of primary olivine are found in Y-86720, and unaltered primary olivine is abundant in B-7904 (TOMEOKA *et al.*, 1989a, b; BISCHOFF and METZLER, 1991). These differences suggest that the degrees of hydrous alteration are quite different among the three. On the other hand, the three unusual chondrites have suffered similar intense heating by metamorphism or shock-impacts after the hydrous alteration (AKAI, 1988, 1990; TOMEOKA *et al.*, 1989a, b; TOMEOKA, 1990a, b).

Y-86720 has a bulk chemical composition between CM and CI chondrites

(KALLEMEYN, 1988; PAUL and LIPSCHUTZ, 1990), but its overall mineralogy is rather similar to CM chondrites and represents the highest degree of alteration among all CM chondrites (TOMEOKA *et al.*, 1989b). However, the detailed petrography has not been presented and the nature of the hydrous alteration itself is not yet clear. The purposes of this study are to present a detailed petrography of Y-86720 and to clarify the hydration reactions.

2. Sample and Analytical Methods

Two thin sections (Y-86720,71-2 and ,73-2) were borrowed from National Institute of Polar Research (NIPR), and the chemical analyses were performed using an electron-probe microanalyser (JEOL, Superprobe 733, accelerating voltage of 15 kV, and sample current of 3–6 nA). The correction methods of BENCE and ALBEE (1968) and standard ZAF were applied for silicates and oxides and for metals and sulfides, respectively.

3. Petrography

3.1. Overall texture

Y-86720 consists of clasts, isolated minerals, and matrix. The components are summarized in Table 1. Clasts show irregular or subrounded outlines, and their sizes range from a few tens of microns to a few millimeters in diameter. The clasts are mineral aggregates showing clear boundaries against the matrix, and consist mainly of dehydrated phyllosilicates, opaque minerals, and carbonates in various amounts. They are classified into two types on the basis of the predominant phases; phyllosilicate-rich clasts and unusual carbonate-phyllosilicate-rich clasts. Completely altered chondrules, found in Y-86720, are classified as phyllosilicate-rich clasts, because continuous gradation in texture and mineralogy is observed between clasts with and without pseudomorphs of chondrules. Some clasts in Y-86720 have accretional dust mantles (BISCHOFF and METZLER, 1991).

Isolated minerals are defined here as euhedral mineral grains or fragmental grains larger than a few microns, which occur directly in the matrix. They are mainly pyrrhotite, Fe-Ni metal, ilmenite, and phyllosilicate. The matrix is composed

Table 1. Components of Y-86720 carbonaceous chondrite.

Clasts	Phyllosilicate-rich clasts Unusual carbonate-phyllosilicate-rich clasts
Isolated minerals	Euhedral pyrrohtite laths Irregular pyrrohtite grains Metal grains Ilmenite grains Phyllosilicate
Matrix	

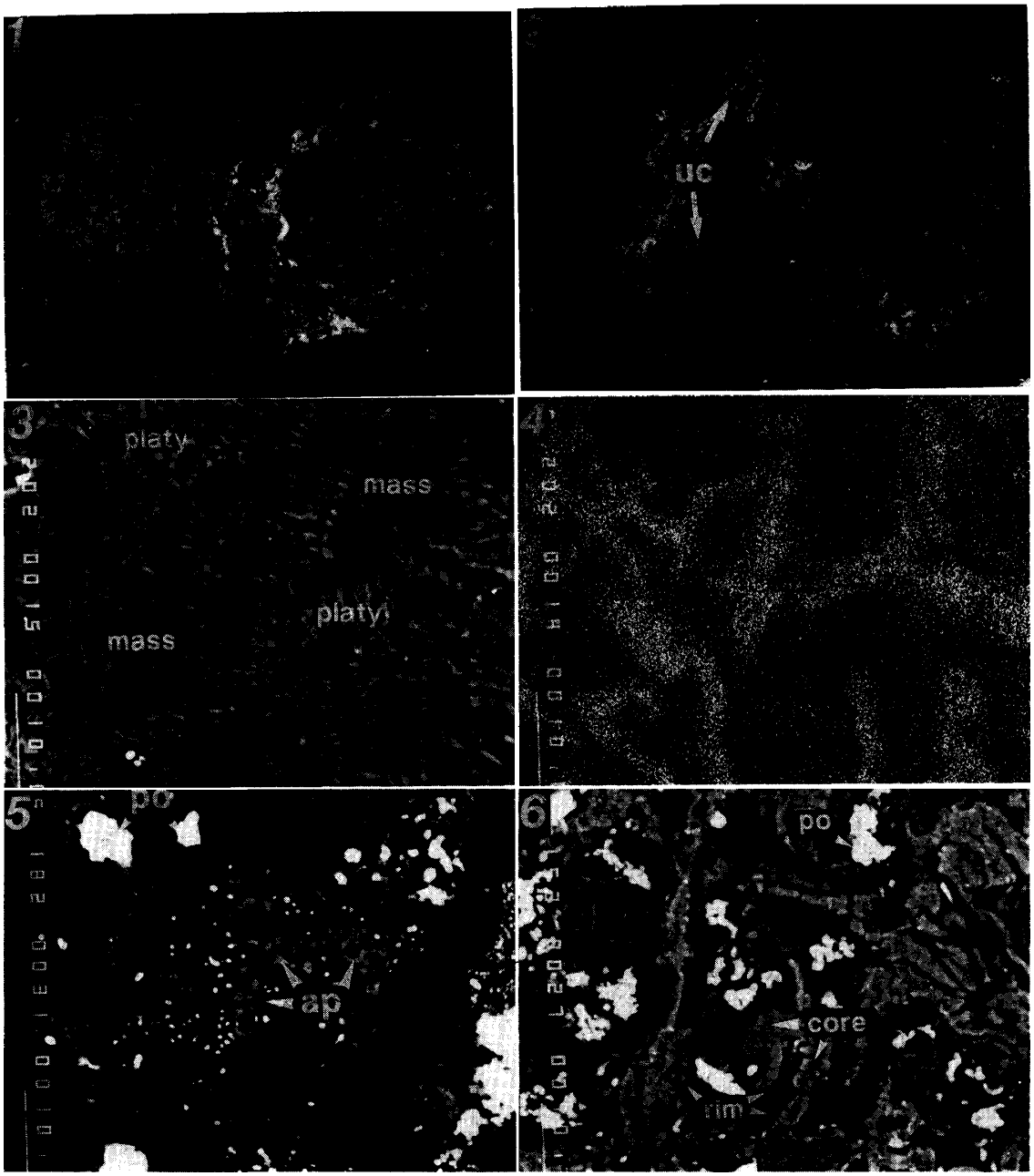

Fig. 1. Photomicrographs of components in Y-86720.

1-1. Photomicrograph of a phyllosilicate-rich clast. Transmitted light, open nicol, 0.9 mm wide.

1-2. Photomicrograph of unusual carbonate-phyllosilicate-rich inclusions (uc) in a phyllosilicate-rich clast. Transmitted light, open nicol, 0.45 mm wide.

1-3. BSE image of typical occurrence of coarse-grained platy (platy) and fine-grained massive (mass) phyllosilicates in a clast.

1-4. X-ray image (Al, K-α line) of the same area shown in Fig. 1-3. Note that massive phyllosilicate shows high Al content.

1-5. BSE image of typical occurrence of apatite (ap) in a clast. po; pyrrhotite.

1-6. BSE image of an unusual carbonate-phyllosilicate inclusion in a phyllosilicate-rich clast. Irregularly-elongated objects denoted by core is a mixture of carbonate and phyllosilicate with minor phosphate, and they are surrounded by a thin rim consisting mainly of carbonate. Pyrrhotite grains (po) set among the mixture.

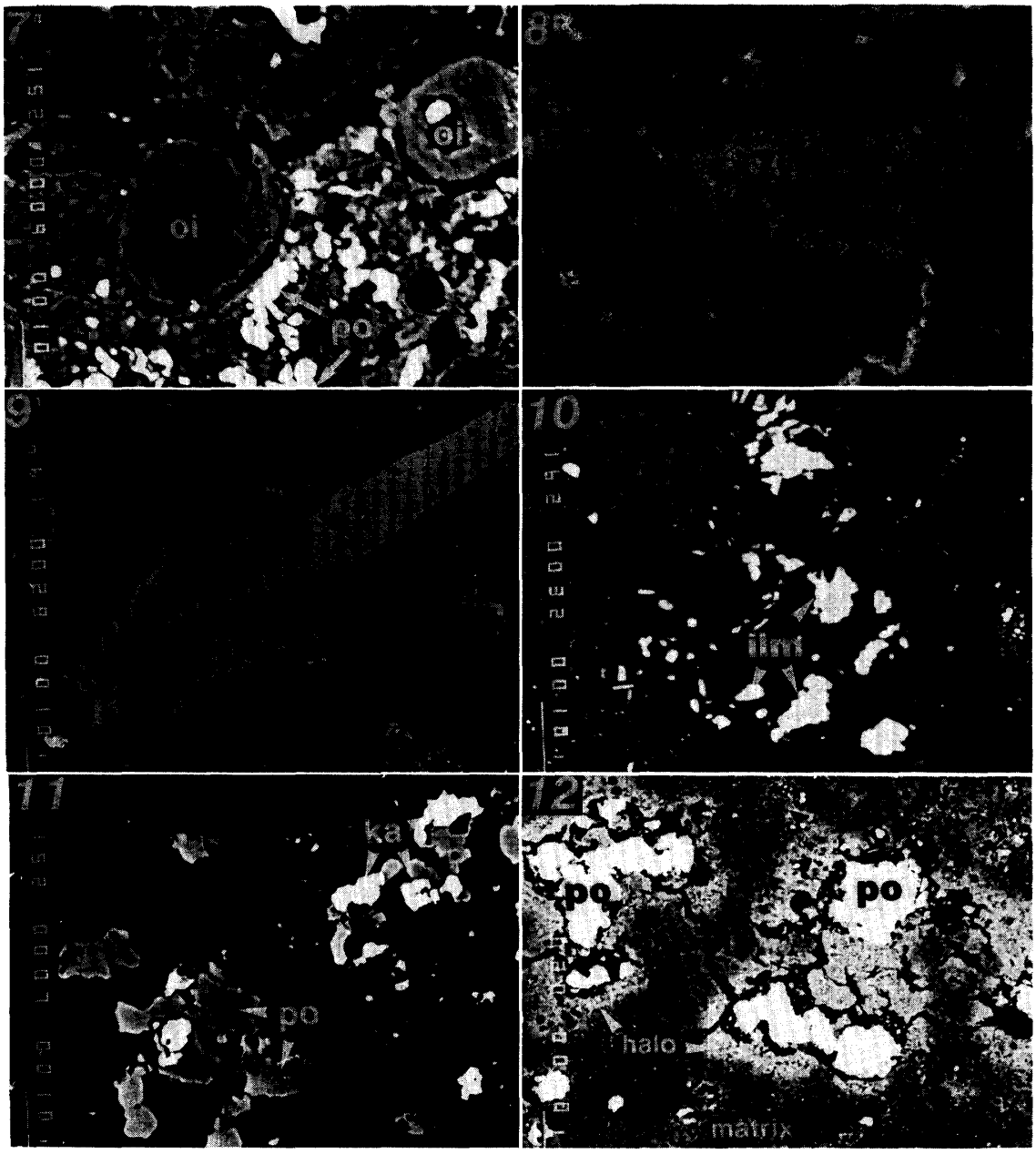

Fig. 1-7. BSE image of ovoidal inclusions (oi) in a clast. Ovoids display a compositional zoning with Fe-rich rim. po; pyrrhotite.

1-8. Photomicrograph of an unusual carbonate-phyllosilicate clast. Transmitted light, open nicol, 0.45 mm wide.

1-9. BSE image of a pyrrhotite lath. Note that the lower left portion of the lath is partially altered to ferrihydrite-like aggregate.

1-10. BSE image of typical occurrence of ilmenite (ilm) in the matrix.

1-11. BSE image of typical occurrence of kamacite (ka) and pyrrhotite (po) in the matrix.

1-12. BSE image of halos around pyrrhotite (po) grains in the matrix.

of aggregates of tiny mineral and mineraloid grains smaller than a few microns, which fill the interstitial spaces between clasts and isolated minerals.

3.2. Phyllosilicate-rich clasts

Phyllosilicate-rich clasts (Figs. 1–1 and 1–2) consist mainly of dehydrated phyllosilicates with variable amounts of opaque minerals, up to about 30 vol%. The opaque minerals are mainly pyrrhotite and taenite, and the minor minerals are ilmenite, kamacite, chromite, and phosphates (apatite and whitlockite). Back-scattered electron (BSE) images reveal that each pyrrhotite grain in phyllosilicate-rich clasts has a bright halo several to a few tens of microns wide. Some phyllosilicate-rich clasts show pseudomorphs of porphyritic olivine chondrules, although anhydrous silicate minerals such as olivine or pyroxene are never found in the clasts. Phyllosilicates show two types of textures; coarse-grained platy and fine-grained massive (Fig. 1–3). Some clasts include variable amounts of Ca-phosphate (Fig. 1–5).

Phyllosilicate-rich clasts sometimes include two kinds of inclusions, unusual carbonate-phyllosilicate inclusions and ovoidal phyllosilicate inclusions. The former consists of fine-grained mixtures of phyllosilicate and carbonate showing an irregular outline (Fig. 1–2). Figure 1–6 shows that the inclusions have an unusual texture, in which an irregularly-elongated object consists of a bright core and a thin rim, always associated with an irregularly shaped pyrrhotite of a few to several microns across.

Ovoidal phyllosilicate inclusions are small spheres, several to several tens of microns across, consisting mainly of fine-grained phyllosilicates (Fig. 1–7). BSE images reveal that ovoidal inclusions in some phyllosilicate-rich clasts show a zonal structure with a dark core and a bright rim (Fig. 1–7). Unzoned ovoidal inclusions consist of either bright or dark material.

3.3. Unusual carbonate-phyllosilicate-rich clasts

Unusual carbonate-phyllosilicate-rich clasts (Fig. 1–8) show an unusual texture

Table 2. Representative chemical compositions of dehydrated phyllosilicates in Y-86720.

	Main Cluster					Massive High-Al	Platy Low-Al
	190	197	607	609	523	538	502
SiO_2	41.03	40.12	44.76	44.03	34.62	38.01	46.52
TiO_2	0.07	0.10	0.17	0.11	0.28	0.30	0.12
Al_2O_3	3.35	2.90	3.80	3.10	19.60	10.47	3.27
Cr_2O_3	0.91	0.54	0.93	0.26	0.70	1.15	1.76
FeO	10.76	10.70	11.62	12.05	15.91	18.40	11.40
MnO	0.17	0.10	0.00	0.00	0.19	0.00	0.00
MgO	30.27	33.72	26.47	32.81	24.38	25.47	28.07
CaO	0.80	0.17	0.60	0.11	0.10	0.00	0.13
Na_2O	0.80	0.71	0.66	0.76	2.74	1.74	0.63
K_2O	0.15	0.13	0.18	0.16	0.14	0.12	0.08
Total	88.31	89.19	89.19	93.39	98.66	95.66	91.98

similar to that of carbonate-phyllosilicate inclusions in some phyllosilicate-rich clasts. The mineral assemblages are similar, therefore, they may have derived from those inclusions by disaggregation of phyllosilicate-rich clasts.

3.4. Isolated minerals

Phyrrhotite, Fe-Ni metal, ilmenite, and phyllosilicate occur as isolated minerals in Y-86720. Pyrrhotite shows two different outlines of grains, irregularly shaped grains and euhedral laths (Fig. 1–9). The irregular pyrrhotite grains are smaller than a few tens of microns, while euhedral pyrrhotite laths are sometimes up to 1000 microns in length. The cores of some pyrrhotite laths are altered to a fine-grained heterogeneous material, probably including ferrihydrite (Fig. 1–9). Ilmenite (Fig. 1–10) and taenite occur as irregular grains, smaller than several microns across. Kamacite occurs rarely in intimate association with pyrrhotite in the matrix (Fig. 1–11).

3.5. Matrix

The matrix consists mainly of fine-grained phyllosilicates with minor amounts of tiny Fe-phases smaller than a few microns. Ca carbonates may be rare in the matrix, because the CaO content of the matrix is low (mainly 0.1–0.3 wt%) but vary heterogeneously when the matrix was analyzed using a focussed beam of an EPMA. BSE images reveal that the matrix surrounding isolated pyrrhotite grains and some clasts including abundant pyrrhotite becomes bright without any textural change, and the bright halos are several to a few tens of microns wide (Fig. 1–12).

4. Mineralogy

The representative chemical compositions of the constituent minerals are shown in Table 2 for dehydrated phyllosilicates and oxides, and in Table 3 for metals and sulfides. Although all phyllosilicates in Y-86720 were dehydrated by a heating event

Ovoidal inclusions are mixtures of dehydrated phyllosilicates and a Fe-bearing phase.

Ovoid core	Ovoid rim	Ovoid	Ovoid	Matrix			
94	99	307	303	476	488	808	809
33.23	27.18	25.27	28.11	33.16	32.53	36.10	37.89
0.05	0.05	0.07	0.07	0.30	0.04	0.14	0.11
4.19	3.06	2.30	2.54	2.74	2.71	2.60	2.82
1.33	1.17	1.24	1.62	0.57	0.56	0.64	0.81
21.31	41.59	44.42	41.42	18.56	18.27	18.83	20.37
0.10	0.00	0.07	0.00	0.19	0.56	0.00	0.00
21.27	17.87	17.00	18.82	23.59	22.35	20.48	23.41
0.17	0.06	0.30	0.06	0.18	0.21	0.25	0.18
0.57	0.07	0.10	0.14	0.46	0.43	0.50	0.57
0.11	0.00	0.00	0.00	0.08	0.13	0.15	0.24
82.33	91.05	90.77	92.78	79.83	77.79	79.69	86.40

Table 3. Representative chemical compositions

	Clast No.6	Clast No. 6	Clast No. 7	Clast No. 17	Clast No. 17	Clast No. 23
Mineral	Pyrrhotite	Kamacite	Taenite	Pyrrhotite	Taenite	Kamacite
Fe	62.92	98.84	35.42	62.29	45.38	95.85
Co	0.04	0.14	2.83	0.08	2.02	0.31
Ni	0.00	0.81	61.40	0.28	50.72	2.85
S	37.10	0.01	0.00	37.50	0.00	0.09
Total	100.06	99.80	99.65	100.15	98.12	99.10

(TOMEOKA *et al.*, 1989b; AKAI, 1990), the original phyllosilicates prior to the dehydration can be speculated from the chemical compositions, and are discussed here.

4.1. Phyllosilicate

As shown in Fig. 2a, chemical compositions of the Y-86720 matrix are fairly homogeneous, concentrating in serpentine (or chlorite) solid solution with mg values between 0.73 and 0.55. Figure 3 indicates that the matrix originally comprised major serpentine (chlorite) and minor sodian talc (or saponite) components. The alkali

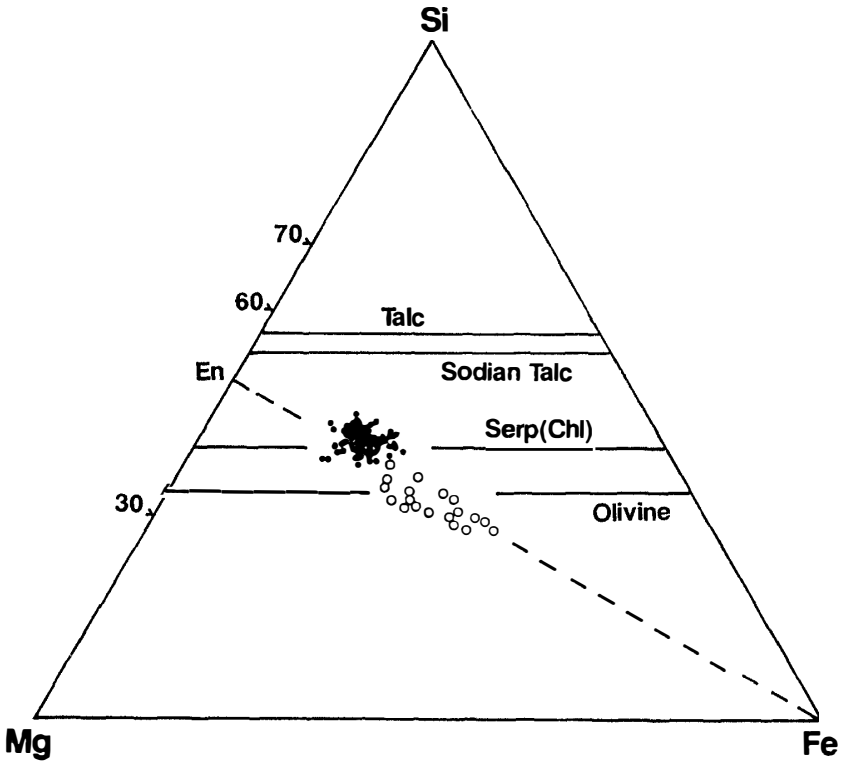

Fig. 2a. Si-Mg-Fe atomic plot of chemical compositions of the Y-86720 matrix. Solid circles are normal matrix, and open circles are halos around pyrrhotite grains in the matrix. Four lines with Talc, Sodian Talc, Serp (Chl) an Olivine are MgO-FeO solid solutions of talc, Na-Al talc, serpentine (or chlorite), and olivine, respectively.

of metals and sulfides in Y-86720.

Clast No. 31	Clast No. 31	Isolated minerals			Lath
Pyrrhotite	Kamacite	Taenite	Pyrrhotite	Kamacite	Pyrrhotite
62.00	96.72	40.81	62.08	95.78	60.79
0.05	0.11	3.16	0.12	0.26	0.05
0.02	1.91	54.61	0.00	2.15	0.05
37.60	0.03	0.07	37.25	0.03	38.66
99.67	98.77	98.65	99.45	98.22	99.56

contents (Na_2O) range from 0.1 to 0.7 wt%, and the Cr_2O_3 content from 0.4 to 0.6 wt% (Fig. 4). The Al_2O_3 content is also homogeneous, ranging from 1.9 to 2.9 wt% (Fig. 4), and the CaO content is low with the range from 0.1 to 0.3 wt%. However, compositions of the halos surrounding pyrrhotite grains in the matrix differ

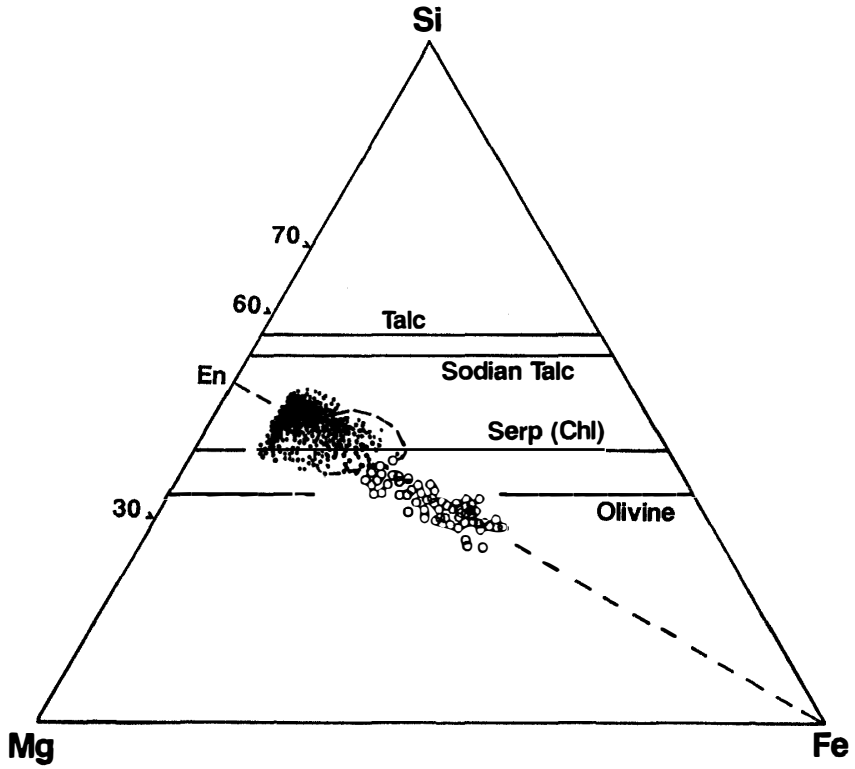

Fig. 2b. Si-Mg-Fe atomic plot of chemical compositions of clast phyllosilicates with the CaO less than 2 wt% (solid circles) and halos around pyrrhotite grains and rims of zoned ovoidal inclusions in clasts (open circles). Compositional range of the matrix is shown by dashed line for reference. Note that most of clast phyllocilicates are plotted along a line of a constant fe/(Si+Mg+Fe) ration of about 0.10, forming a main cluster, and that halos around pyrrhotite grains are plotted in an Fe-rich portion along a dashed tie line connecting enstatite (En) with the Fe apex. Four lines with Talc, Sodian Talc, Serp (Chl) and Olivine are MgO-FeO solid solutions of talc, Na-Al talc, serpentine (or chlorite), and olivine, respectively.

from the normal matrix as shown in Fig. 2. The halos are more or less enriched in Fe.

Phyllosilicates in all phyllosilicate-rich clasts are plotted in Fig. 2b, which indicates that phyllosilicate in clasts was mixtures of serpentine (or chlorite) and sodian talc (or saponite). But the phyllosilicates in clasts differ in chemical compositions from those in the matrix, although the compositional ranges overlap as shown in Fig. 2b. They are richer in Al, Si, Mg, and alkalis, and poor in Fe on the average than those in the matrix, meaning that the phyllosilicates in clasts were originally more enriched in sodian talc (or saponite) component on the average than those in the matrix. In contrast to the constant Al_2O_3 content of the matrix phyllosilicates, the Al_2O_3 content of clast phyllosilicates ranges from 1.5 to 20 wt% (Fig. 4). As shown in Fig. 1–4, fine-grained massive phyllosilicates are high in Al_2O_3 content (6.6–20 wt%), and phyllosilicates showing a coarse-grained platy texture are low in the content (1.5–6.5 wt%).

In Fig. 2b, most of the clast phyllosilicates plot parallel to a line with a constant Fe/(Si+Mg+Fe) atomic ratio of about 0.1, forming a main cluster, although minor phyllosilicates in clasts are distributed from the main cluster toward the Fe apex,

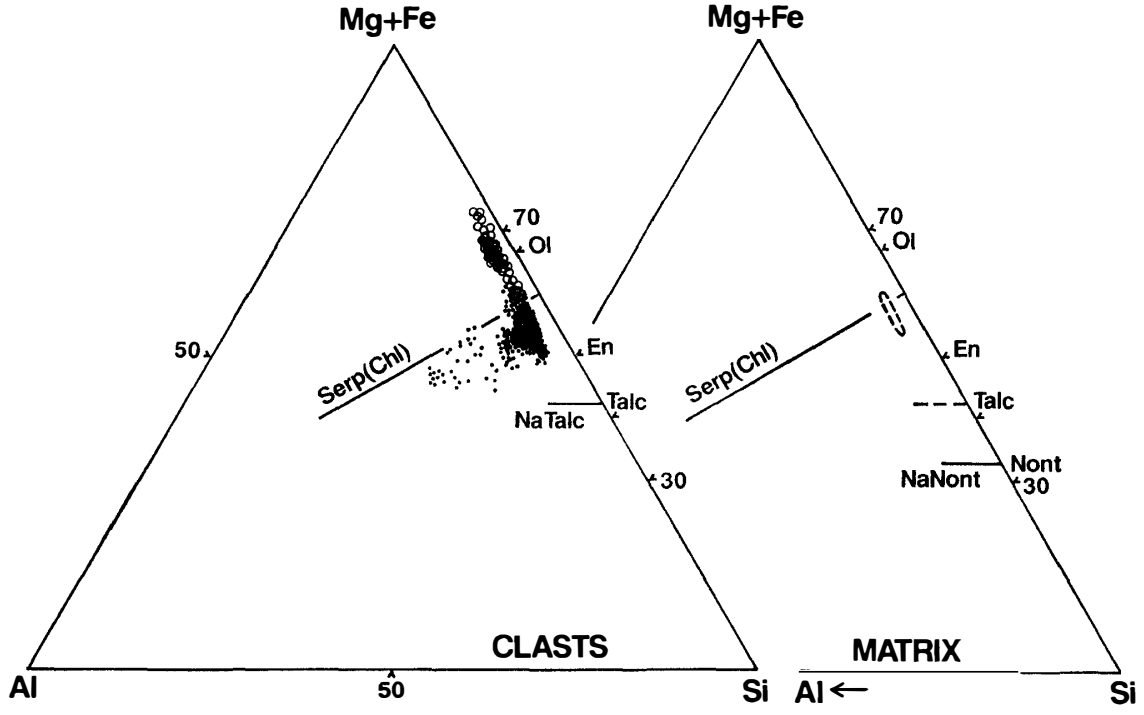

Fig. 3. (Mg+Fe)-Al-Si atomic plot of chemical compositions of clast phyllosilicates with the CaO less than 2 wt% (solid circles) and halos around pyrrhotite grains and some ovoidal inclusions (open circles) in clasts. Compositional range of the matrix is shown by a dashed circle in the right hand triangle for reference. Note that most of low-Al phyllosilicates in clasts are plotted along a line connecting sodian talc (or saponite) component with low-Al serpentine (chlorite), that high-Al phyllosilicates in clasts are plotted in the talc component-richer portion than the serpentine (or chlorite) solid solution (Serp (Chl)), and that the halos and some ovoidal inclusions are plotted in an Si-pooer portion than the serpentine (or chlorite) solid solution. NaTalc, Nont, and NaNont are Na-Al talc, nontronite $\{Fe_4Si_8O_{20}(OH)_4\}$, and Na-Al nontronite $\{NaFe_4Si_7AlO_{20}(OH)_4\}$, respectively.

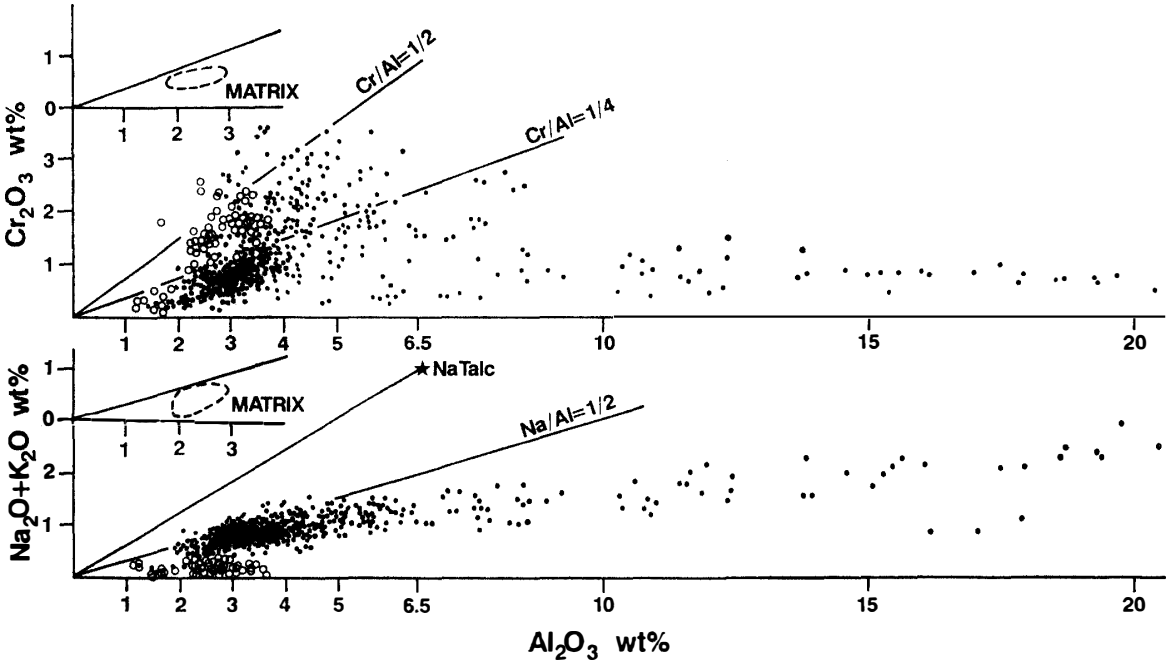

Fig. 4. Alkalis and Cr_2O_3 contents (wt%) of clast phyllosilicates with the CaO less than 2 wt% (solid circles) and halos around pyrrhotite grains and some ovoidal inclusions (open circles) in clasts are plotted against the Al_2O_3 content (wt%). Compositional range of the matrix is shown by a dashed circle for reference. Note that the halos and some ovoidal inclusions are low in alkali contents, and that the alkali contents of most low-Al (Al_2O_3<6.5 wt%) phyllosilicates are plotted along a line with Na/Al atomic ratio of 0.5. A star with NaTalc shows the chemical composition of stoichiometric Na-Al talc {$NaMg_6Si_7AlO_{20}(OH)_4$}.

resulting in overlap with those in the matrix. In Fig. 5, phyllosilicates in two phyllosilicate-rich clasts (Nos. 17 and 110) are plotted along a tie line T-S, and they all belong to the main cluster. This suggests that the main cluster corresponds in chemical composition to mixtures of sodian talc (or saponite) component T and serpentine (chlorite) component S, and that the two components T and S may have been equilibrated in the clasts. If so, sodian talc (or saponite) component T is more ferroan and richer in Al than the coexisting serpentine (or chlorite) component S (Fig. 5). The partition coefficient of MgO and FeO between the two components T and S, K_{Mg-Fe} ($=X_{Mg}/X_{Fe}$ ratio of component T divided by X_{Mg}/X_{Fe} ratio of component S, where X is mole fraction), is about 0.59, on an assumption that all the Fe in the phyllosilicates existed as Fe^{2+}. The partition coefficient of Al between the two components T and S, K_{Al} (Al content of component T divided by Al content of component S), is about 2.5.

The halos surrounding pyrrhotite grains in phyllosilicate-rich clasts were analyzed using a focussed beam to avoid the tiny opaque grains, and the chemical compositions obtained are shown in Fig. 2b. They are more Fe-rich than those in the normal matrix, but are similar to the halos in the matrix (Fig. 2a). This indicates that the halos are a mixture of phyllosilicate and a submicroscopic Fe-bearing phase (Fe-oxide, Fe-hydroxide, Fe-sulfides, or Fe-metal). In addition, the halos are poorer in alkalis than the normal clast phyllosilicates (Fig. 4).

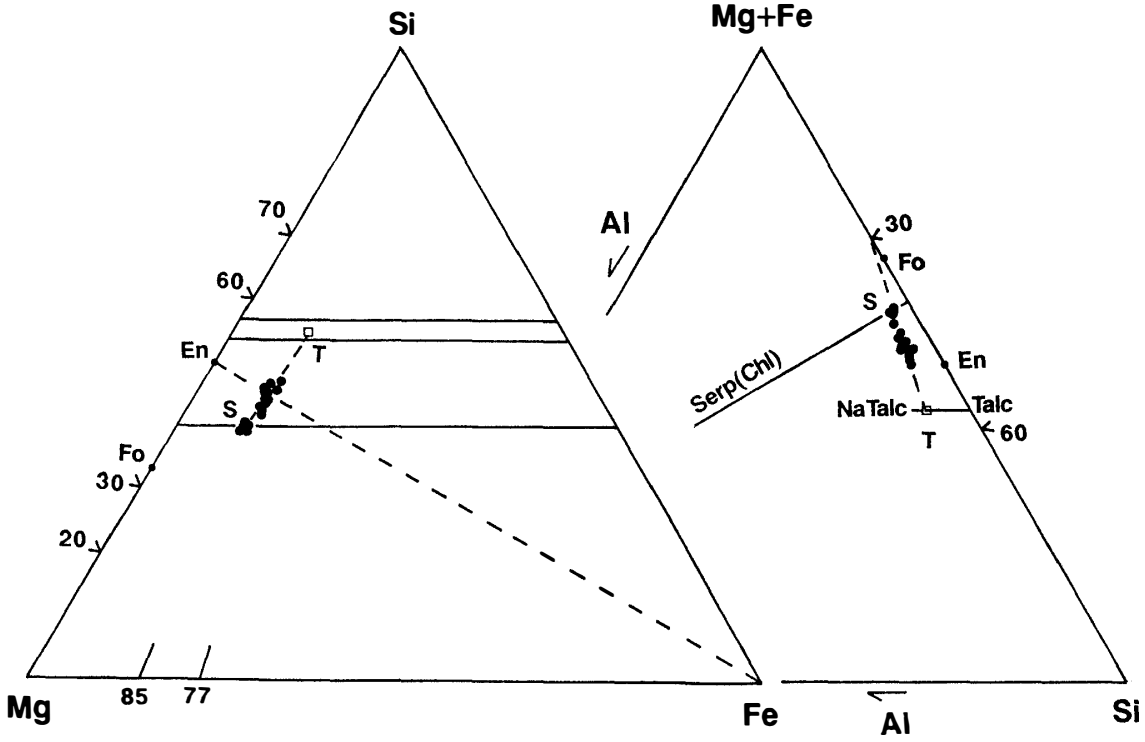

Fig. 5. Composition of phyllosilicates of clast Nos. 17 and 110, which correspond to the main cluster. Note that the phyllosilicates are a mixture of two components, sodian talc (or saponite) T and serpentine (or chlorite) S.

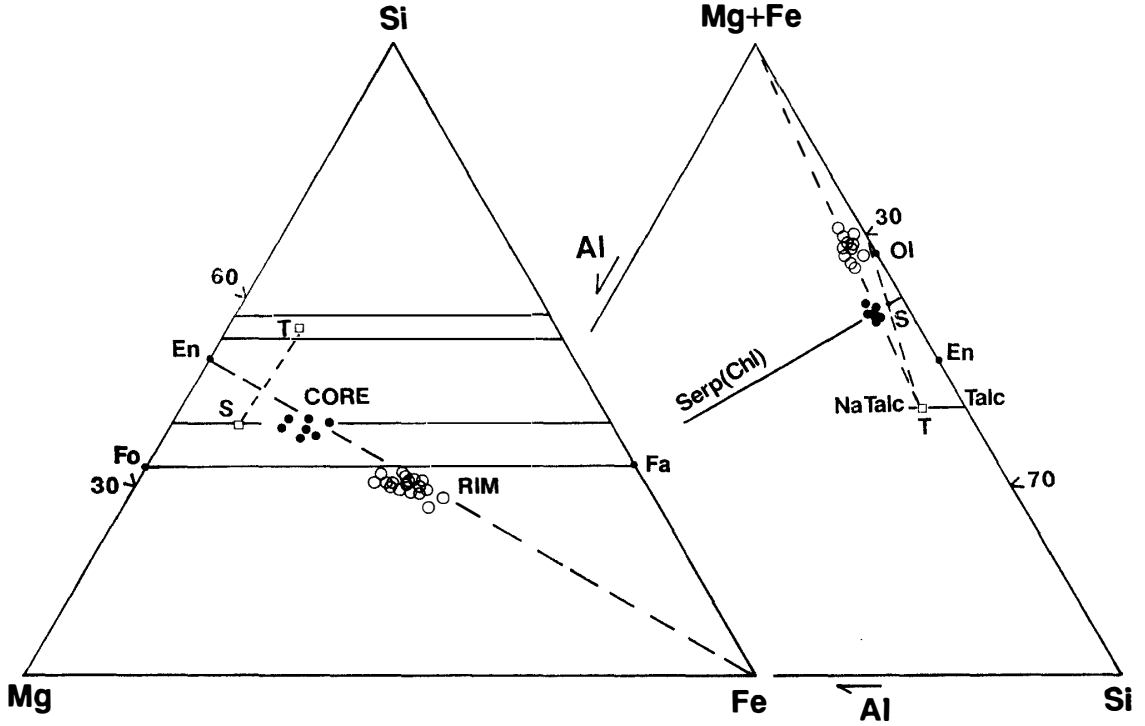

Fig. 6. Chemical compositions of core and rim of zoned ovoidal inclusions in clast No. 6. The core is serpentine (or chlorite), and the rim is a mixture of the phyllosilicates and an Fe-bearing phase.

Ovoidal inclusions in some phyllosilicate-rich clasts show a zonal structure, and the chemical compositions of cores and rims of zoned ovoidal inclusions in clast No. 6 are shown in Fig. 6. The core is chemically serpentine (or chlorite) similar to those in the normal matrix, but the rim is extremely enriched in Fe, indicating that the rim is a mixture of the core phyllosilicate and a submicroscopic Fe-bearing phase. Some ovoidal inclusions without zonal structure are similar in chemical composition to the rim of zoned ovoidal inclusions, but others are similar to the core of zoned ovoidal inclusions or to phyllosilicate of the main cluster.

4.2. Fe-Ni metal

Fe-Ni metal occurs in phyllosilicate-rich clasts and as isolated minerals, and it is kamacite and taenite. Kamacite occurs in intimate association with troilite in some clasts, and taenite occurs in association with troilite in other clasts, although rarely they coexist in a same clast. Compositions of Fe-Ni metals are shown in Fig. 7. The Ni content of taenite extends up to 62 wt%, suggesting that some grains may be awaruite. Most of taenite is rich in Ni and Co and plots near the line with the Co/Ni ratio of solar composition, but kamacite is poor in Co and Ni plots slightly above the solar composition line (Fig. 7). A few kamacite grains in some phyllosilicate-rich clasts are rich in Co, up to 4 wt%, and are sometimes associated with Co-poor taenite (Fig. 7).

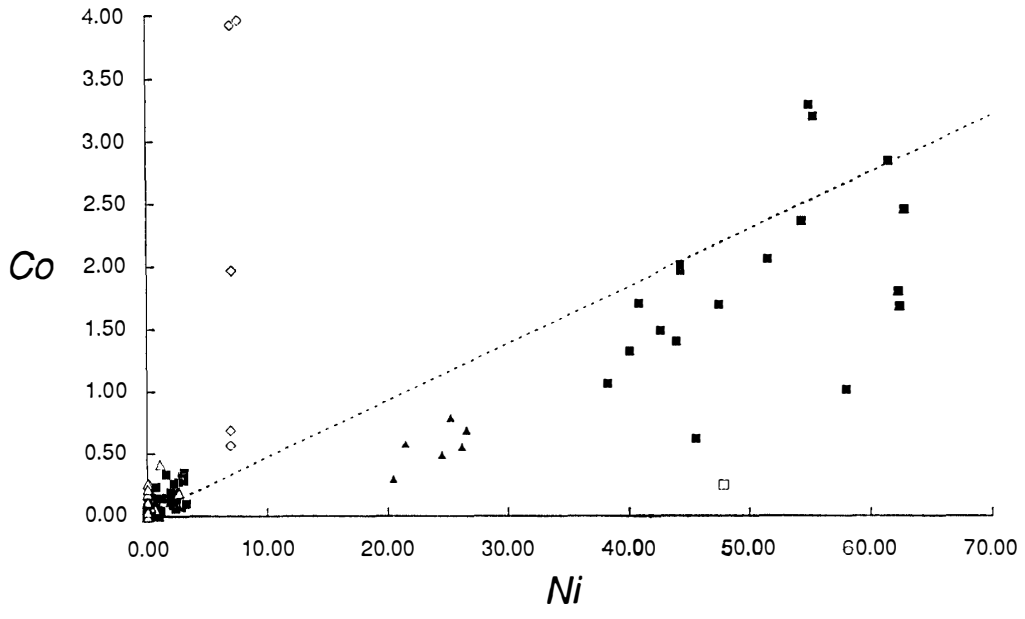

Fig. 7. Nickel and cobalt contents (wt%) of metals and sulfides. A dashed line indicates Co/Ni ratio of the solar composition. Solid squares: Ni-Co-poor kamacite and Ni-Co-rich taenite, open dias: Co-rich kamacite, open squares: taenite coexisting with Co-rich kamacite, solid triangles: pentlandite, and open triangles: pyrrhotite.

4.3. Sulfide

Sulfide is mostly pyrrhotite, and rarely pentlandite. The average composition of pyrrhotite is $Fe_{0.95}S$. Pentlandite occurs as small grains in large euhedral troilite

laths, and the size is less than several microns. The Ni content of pentlandite ranges from 20 to 28 wt% (Fig. 7).

4.4. *Ilmenite*

Ilmenite occurs in some clasts and as an isolated mineral. The chemical composition is 54–55 TiO_2 wt%, 39–41 FeO wt%, 0.4–0.6 MnO wt%, and 4–5 MgO wt%. The atomic ratio of (Fe+Mn+Mg)/Ti is nearly unity, suggesting that ilmenite is nearly free from a hematite component.

4.5. *Carbonate*

Carbonate is too small to be observed under a SEM and to obtain its chemical composition by an EPMA. However, the existence of Ca carbonate is suggested by EPMA analyses. The chemical compositions of components of unusual inclusions and clasts, which were obtained by a focused beam, are plotted in Fig. 8. The figure suggests that the unusual inclusions and clasts consist mainly of fine-grained mixtures of phyllosilicates and Ca carbonate with a minor amount of Ca phosphate.

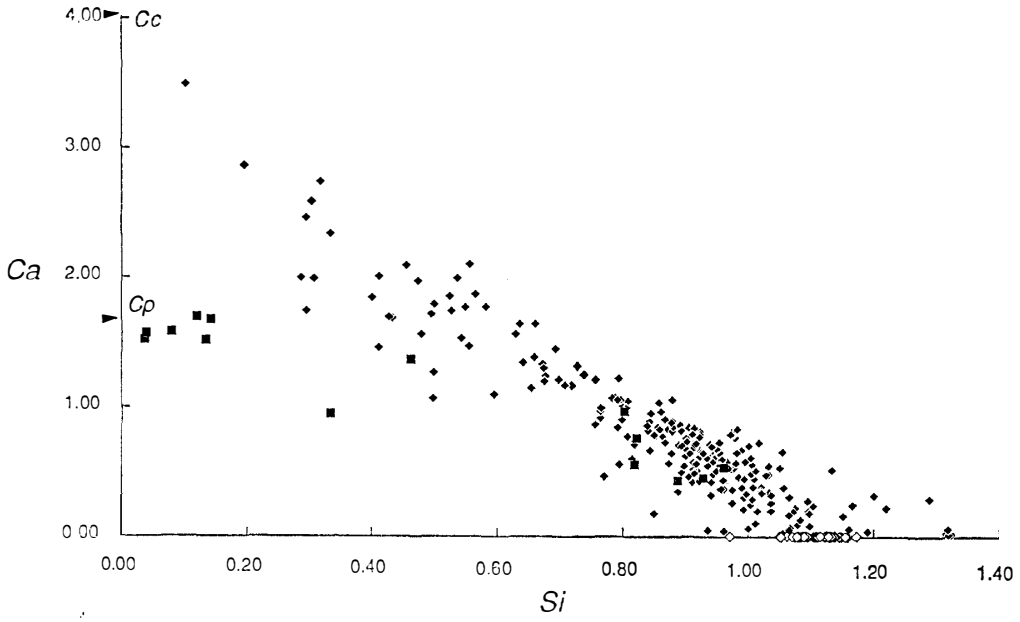

Fig. 8. Silicon and Ca atomic contents of unusual carbonate-phyllosilicate inclusions normalized by O=4. Ca contents of Ca-carbonate (Cc) and Ca-phosphate (Cp) are indicated by arrows. Note that carbonate-phyllosilicate inclusions are a mixture of Ca-carbonate and phyllosilicate with a small amount of Ca-phosphate. Solid dias: unusual carbonate-phyllosilicate inclusions, solid squares: those including P more than 0.1 (normalized by O=4), and open dias: phyllosilicate in the matrix.

4.6. *Others*

Phosphate occurs in some clasts and the matrix (Fig. 1–5), and the size is smaller than a few microns. Phosphates rarely contain Na_2O up to 1.5 wt%, and sometimes chlorine is qualitatively detected in small amounts, suggesting that they are both whitlockite and chlorapatite. In addition, a small amount of phosphate

seems to occur in some unusual carbonate-phyllosilicate inclusions and clasts, because minor P_2O_5 is detected in addition to CaO. It is Ca-phosphate (Fig. 8). Ferrihydrite-like material occurs in the central portion of some euhedral pyrrhotite laths and sometimes at the rims (Fig. 1–9). Chromite, several microns across, occurs in some clasts, and its composition is: 15–17 Al_2O_3 wt%, 1.0–1.1 TiO_2 wt%, 48–49 Cr_2O_3 wt%, 25 MgO wt%, 7.1–7.5 FeO wt%, and 0.3 MnO wt%.

5. Discussion

5.1. Hydration of phyllosilicate-rich clasts

Phyllosilicate in some phyllosilicate-rich clasts shows two different textures, coarse-grained platy and fine-grained massive. Aggregates of the coarse-grained platy phyllosilicate show outlines similar to those of pyroxene or olivine grains in unaltered chondrules of other CM chondrites, and the occurrence of fine-grained massive phyllosilicate aggregates resembles the glassy groundmass of unaltered chondrules (Figs. 1–3 and –4). The two types of phyllosilicates that are similar to those in Y-86720 occur in large chondrules of B-7904, and IKEDA *et al.* (1991) concluded that the fine-grained massive and coarse-grained platy phyllosilicates were produced by hydration mainly from plagioclase and pyroxene, respectively. Therefore, the Y-86720 clasts, including the two phyllosilicate types, were originally chondrules consisting mainly of olivine, pyroxene, and plagioclase (and/or mesostasis glass rich in plagioclase component), and the chondrules have undergone complete hydration to produce fine-grained massive phyllosilicates mainly from plagioclase or mesostasis, and coarse-grained platy phyllosilicates mainly from pyroxene and probably olivine.

5.2. Halos around FeS grains

Halos surrounding pyrrhotite grains are commonly observed in the matrix and in clasts including FeS grains. TOMEOKA *et al.* (1989b) already reported halos in Y-86720, but they did not discuss the origin. The halos are enriched in Fe as shown in Fig. 2, indicating that they are mixtures to phyllosilicate and an Fe-bearing phase. As the sulfur content of halos is below the detection limit, the Fe-bearing phase may be Fe-oxide, Fe-hydrate, or metallic Fe. The low alkali contents of halos (Fig. 4) indicate that alkalis were leached from the halos during the formative period.

It is evident that the halos were produced by alteration of pyrrhotite after the agglomeration of the Y-86720 chondrite. The idea that the halos were produced by terrestrial alteration of FeS in Antarctica seems improbable, because small Co-Ni-poor kamacite grains, which are considered to alter more easily than FeS by the terrestrial weathering, remain unaltered in the matrix. Therefore, they had formed prior to the formation of Co-Ni-poor kamacite. As the Co-Ni-poor kamacite may have formed by a heating event in the parent body, as discussed later, the formation of halos must have taken place in the parent body after the agglomeration and prior to the heating event. Probably, they were produced by aqueous alteration of pyrrhotite in the parent body.

5.3. Ovoidal phyllosilicate inclusions in clasts

Ovoidal inclusions in some phyllosilicate-rich clasts are similar in size and occurrence to metal inclusions commonly occurring in olivine phenocrysts of unaltered chondrules in other CM chondrites. They may have been produced by hydration from metal grains in original chondrules, and their compositions may have been similar to the main cluster phyllosilicates or the matrix phyllosilicates. Zoned ovoidal inclusions have rims enriched in Fe, caused by dissemination of an FeO-bearing phase during the alteration of pyrrhotite, which resulted in the halos around the pyrrhotite grains.

5.4. Unusual carbonate-phyllosilicates inclusions in some clasts, and unusual carbonate-phyllosilicate-rich clasts

These inclusions and clasts show unusual textures (Fig. 1–6) which have never been found in other carbonaceous chondrites. The inclusions always contain many FeS grains which are surrounded by fine-grained mixtures of carbonate and phyllosilicate. The occurrence of unusual inclusions in some clasts (Fig. 1–2) suggests that they may have been troilite grains included in original chondrules. This is suggested by the fact that original troilite in chondrules was replaced by carbonate and phyllosilicate during the alteration of chondrules.

Generally, hydration of chondrules in other CM chondrites expelled the original CaO outside chondrules (IKEDA, 1983; IKEDA *et al.*, 1991). However, the hydration of Y-86720 retained CaO within chondrules as unusual inclusions. This is consistent with the fact that the Y-86720 matrix is depleted in CaO in comparison to the B-7904 and Y-82162 matrices, where the CaO was expelled from chondrules during the alteration of chondrules and precipitated as carbonates or phosphates in the matrices (IKEDA *et al.*, 1991; KIMURA and IKEDA, 1992).

5.5. Multi-stage hydration

The hydration to produce phyllosilicates in clasts and matrix for Y-86720 may have occurred through four stages. Stage (I) was characterized by hydration reactions of pyroxene and plagioclase components in original chondrules to produce phyllosilicates consisting of both sodian talc (or saponite) and serpentine (or chlorite) components (IKEDA *et al.*, 1991). Two kinds of phyllosilicates, low-Al coarse-grained platy and high-Al fine-grained massive were produced in this stage.

Metal grains in original chondrules have also undergone hydration and/or sulfurization during stage (I), and changed their composition by the equation

$$\underset{\text{Ka}}{(\text{Fe, Ni, Co})} + \underset{\text{Ta}}{(\text{Ni, Fe})} + H_2S \longrightarrow \underset{\text{Ta}}{(\text{Ni, Fe, Co})} + \underset{\text{Pyrr}}{FeS} + H_2, \qquad (1)$$

or

$$\underset{\text{Ka}}{2(\text{Fe, Ni, Co})} + H_2O \longrightarrow FeO + \underset{\text{Ta}}{(\text{Ni, Fe, Co})} + H_2, \qquad (2)$$

where Ka, Ta, and Pyrr are kamacite, taenite, and pyrrhotite, respectively, and FeO in the products of eq. (2) becomes a component of phyllosilicates. Most of the

taenite in Y-86720 clasts has Co/Ni ratios similar to the solar composition (Fig. 6), indicating that the taenite was produced by eq. (1) or (2). If a small amount of kamacite in the reactants remained as a relic mineral, the kamacite may have been enriched in Co in comparison with the coexisting taenite (AFIATTALAB and WASSON, 1980). Therefore, Co-rich kamacite and Co-poor taenite in some clasts (Fig. 7) are considered to be relic.

Stage (II) involved hydrous reactions of olivine in chondrules to produce serpentine-rich phyllosilicates, which took place after stage (I) (IKEDA *et al.*, 1991). Phyllosilicates in pseudomorphs after olivine grains were produced in this stage. The chemical compositions of phyllosilicates already produced in stage (I) may have been mostly modified in stage (II), although the Al content of phyllosilicates already produced in stage (I) may not have been completely homogenized in some clasts, because they are the most difficult to be redistributed (IKEDA *et al.*, 1991). The completion of hydrous reactions of stage (II) resulted in an equilibrated assemblage of major serpentine (or chlorite) and minor sodian talc (or saponite) in most clasts, forming the main cluster of phyllosilicates in Y-86720. The ratios of serpentine (or chlorite) component to sodian talc (or saponite) component in clasts varied according to the bulk compositions of original chondrules; olivine-rich chondrules became phyllosilicate-rich clasts enriched in serpentine (or chlorite), and olivine-poor chondrules resulted in clasts enriched in sodian talc (or saponite).

All metal spherules, which are often included in olivine phenocrysts of chondrules in other CM chondrites, have altered during stage (II) to ovoidal phyllosilicate inclusions, because the phyllosilicates in some ovoidal inclusions had chemical compositions similar to the main cluster in stage (II) prior to formation of the zonation.

The CaO contents of original chondrules were retained as unusual carbonate-phyllosilicate inclusions in the clasts during stages (I) and (II), and the unusual inclusions may have been produced from troilite in the original chondrules.

Stage (III) produced the matrix phyllosilicates, which are homogeneous in chemical composition except for the Si content (Fig. 3). Chemical compositions of the matrix phyllosilicates plot along a line of constant Al, as shown in Fig. 3, indicating that they are mixtures of serpentine (or chlorite) and sodian talc (or saponite) components. However, the line of constant Al is slightly oblique to the main cluster trend S-T in Fig. 5, suggesting that the mixture of the matrix is different in mineral assemblage from mixtures of the main cluster phyllosilicates. Although the crystallographic structure of phyllosilicates in Y-86720 has been completely destroyed by a later heating event (AKAI, 1990; TOMEOKA *et al.*, 1989b), TOMEOKA *et al.* (1989b) suggested that the matrix phyllosilicates are mixtures of serpentine and smectite-type phyllosilicate. In this case, we can show a possible equation for the mixtures from the talc component already produced;

$$\underset{\text{Talc}}{2Mg_6Si_8O_{20}(OH)_4} + \underset{\text{Pyrr}}{4FeS} + 12H_2O \longrightarrow$$

$$\underset{\text{Serp}}{Mg_{12}Si_8O_{20}(OH)_{16}} + \underset{\text{Nont}}{Fe_4Si_8O_{20}(OH)_4} + 4H_2S + 2H_2\,, \qquad (3)$$

where Nont is nontronite, which is ferric dioctahedral saponite. Terrestrial nontronite usually includes small amounts of Ca and alkalis, being consistent with low contents of CaO and alkalis in the matrix phyllosilicates of Y-86720 (Table 2 and Fig. 4). Equation (3) means that ferric saponite became stable instead of talc, because of the low-temperature reaction. Recently, SCORZELLI and SOUZA AZEVEDO (1991) carried out a Mössbauer spectroscopy study on Y-86720, and detected probable Fe^{3+} in the matrix. The Fe^{3+} may be partly due to the nontronite component. In stage (III), all talc component in precursors of the matrix was consumed to produce the homogeneous mixtures of major serpentine and minor nontronite of the Y-86720 matrix. In addition, the main cluster phyllosilicates in some clasts more or less changed their compositions by eq. (3), resulting in overlap in composition with the matrix phyllosilicates.

As already stated in the preceding sections, pyrrhotite in clasts and matrix has a halo, which consists of mixtures of phyllosilicates and an Fe-bearing phase. Stage (IV) was the formation of the Fe-bearing phase. A possible reaction for formation of the Fe phase is;

$$\underset{\text{Pyrr}}{2FeS} + 6H_2O \longrightarrow \underset{\text{Ferri}}{2Fe(OH)_3} + 2H_2S + H_2 , \qquad (4)$$

where Pyrr and Ferri are pyrrhotite and ferrihydrite, respectively. The ferrihydrite component produced by eq. (4) may have been disseminated into the surrounding phyllosilicates, resulting in the halos around the pyrrhotite grains. The brown rims of ovoids were also produced by dissemination of the ferrihydrite component supplied from outside the ovoids, resulting in mixtures of ferroan serpentine and the Fe-bearing phase. Stage (IV) must have taken place after the final aggregation of the chondrite, because the halos are often observed in the matrix.

5.6. *Heating of Y-86720*

Y-86720 suffered intense heating in the last stage, which dehydrated all phyllosilicates. AKAI (1990) and TOMEOKA *et al.* (1989b) reported that the dehydrated phyllosilicates lost their crystallographic structure and some phyllosilicate grains include submicroscopic olivine and spinel grains which were transformed from the phyllosilicates.

Some clasts and the matrix include small grains of Ni- and Co-poor kamacite (Fig. 7), smaller than 10 microns across, set in the dehydrated phyllosilicates. Considering that all primary olivines have altered to phyllosilicates in Y-86720, it is difficult to see how kamacite grains have survived. Therefore, the Ni- and Co-poor kamacite grains may have been produced by heating from ferrihydrite grains (TOMEOKA *et al.*, 1989b), which were produced by complete reaction of eq. (4). A possible reaction is as follows;

$$\underset{\text{Ferri}}{Fe(OH)_3} \longrightarrow \underset{\text{Ka}}{Fe} + 3/2H_2O + 3/4O_2 , \qquad (5)$$

where Ka is kamacite. Kamacite in the products must be poor in Ni and Co, because troilite in eq. (4) was poor in Ni and Co. Ferrihydrite in halos around pyrrhotite grains in clasts and matrix may have changed to tiny kamacite grains.

5.7. Genetical relationship between Y-86720 and CM or CI chondrites

Non-Antarctic CI chondrites have matrices consisting mainly of serpentine and saponite, although the matrices of CM chondrites are mainly serpentine (TOMEOKA and BUSECK, 1985). Therefore, Y-86720 is similar in matrix mineralogy to CI chondrites. However, the clasts in Y-86720 include large amounts of high-Al phyllosilicates (probably chlorite), which are common in CM chondrites (IKEDA, 1980, 1983), suggesting that Y-86720 is similar in clast mineralogy to CM chondrites. Therefore, Y-86720 has mineralogical characteristics of both CI and CM groups. The bulk chemical composition of Y-86720 also suggests that it is intermediate between CI and CM groups (KALLEMEYN, 1988; PAUL and LIPSCHUTZ, 1990). The oxygen isotopic composition of the Y-86720 whole rock also indicates that Y-86720 is located at a critical point crossing the CM mixing line with terrestrial mass fractionation line on which CI group is plotted (MAYEDA *et al.*, 1991). Conclusively, mineralogy, bulk chemical composition, and oxygen isotopic data indicate that Y-86720 is intermediate between CI and CM groups.

6. Conclusions

(1) Phyllosilicate-rich clasts in Y-86720 consist mainly of serpentine (or chlorite) and sodian talc (or smectite) components, which are homogeneous in chemical composition, in contrast with those in other CM chondrites. This observation suggests that the phyllosilicate clasts have undergone the most intense hydrous alteration.

(2) Metal spherules and troilite grains in original chondrules have also altered to ovoidal phyllosilicate inclusions and unusual carbonate-phyllosilicate inclusions, respectively, which occur commonly in phyllosilicate clasts.

(3) The low-CaO content of the Y-86720 matrix is consistent with the formation of unusual carbonate-phyllosilicate inclusions within clasts. The matrix differs in composition from clast phyllosilicates, suggesting that the two were produced under different conditions. The matrix phyllosilicate may have been a mixture of serpentine and nontronitic smectite.

(4) Halos surrounding pyrrhotite grains in clasts and matrix were produced by the alteration of pyrrhotite, probably to ferrihydrite, after the agglomeration of the Y-86720 chondrite and prior to the heating event, which resulted in hydration of all phyllosilicates and reduction of ferrihydrite to Co-Ni-poor metal.

Acknowledgments

We thank Drs. K. YANAI and H. KOJIMA of National Institute of Polar Research for the sample preparation. This study was supported by a Grant-in-Aid for Scientific Research from Ministry of Education, Science and Culture (to Y. IKEDA).

References

AFIATTALAB, F. and WASSON, J. T. (1980): Composition of the metal phases in ordinary chondrites: Implications regarding classification and metamorphism. Geochim. Cosmochim.

Acta, **44**, 431–446.
AKAI, J. (1988): Incompletely transformed serpentine-type phyllosilicates in the matrix of Antarctic CM chondrites. Geochim. Cosmochim. Acta, **52**, 1593–1599.
AKAI, J. (1989): Mineralogical evidence of heating events in carbonaceous chondrites, Y-82162 and Y-86720. Papers Presented to the 14th Symposium on Antarctic Meteorites, June 6–8, 1989. Tokyo, Natl Inst. Polar Res., 22–23.
AKAI, J. (1990): Mineralogical evidence of heating events in Antarctic carbonaceous chondrites, Y-86720 and Y-82162. Proc. NIPR Symp. Antarct. Meteorites, **3**, 55–68.
BENCE, A. E. and ALBEE, A. L. (1968): Empirical correction factors for the electron microanalysis of silicates and oxides. J. Geol., **76**, 382–403.
BISCHOFF, A. and METZLER, K. (1991): Mineralogy and petrography of the anomalous carbonaceous chondrites Yamato-86720, Yamato-82162, and Belgica-7904. Proc. NIPR Symp. Antarct. Meteorites, **4**, 226–246.
IKEDA, Y. (1980): Petrology of Allan Hills-764 chondrite (LL3). Mem. Natl Inst. Polar Res., Spec. Issue, **17**, 50–82.
IKEDA, Y. (1983): Alteration of chondrules and matrices in the four antarctic carbonaceous chondrites ALH-77307 (C3), Y-790123 (C2), Y-75293 (C2), and Y-74662 (C2). Mem. Natl Inst. Polar Res., Spec. Issue, **30**, 93–108.
IKEDA, Y. (1991): Petrology and mineralogy of the Yamato-82162 chondrite (CI). Proc. NIPR Symp. Antarct. Meteorites, **4**, 187–225.
IKEDA, Y., MAYEDA, T. K., CLAYTON, R. N. and PRINZ, M. (1991): Petrography and oxygen isotopic compositions of chondrules, clasts, and matrix separated from B-7904 and Yamato-86720 carbonaceous chondrites. Papers Presented to the 16th Symposium on Antarctic Meteorites, June 5–7, 1991. Tokyo, Natl Inst. Polar Res., 82–84.
KALLEMEYN, G. W. (1988): Compositional study of carbonaceous chondrites with CI-CM affinities. Papers Presented to the 13th Symposium on Antarctic Meteorites, June 7–9, 1988. Tokyo, Natl Inst. Polar Res., 132–134.
KIMURA, M. and IKEDA, Y. (1992): Mineralogy and petrology of anomalous Belgica-7904: Genetic relationships between the components. Proc. NIPR Symp. Antarct. Meteorites, **5**, 72–117.
MAYEDA, T. K. and CLAYTON, R. N. (1990): Oxygen isotopic compositions of B-7904, Y-82162, and Y-86720. Papers Presented to the 15th NIPR Symposium on Antarctic Meteorites, May 30–June 1, 1990. Tokyo, Natl Inst. Polar Res., 196–197.
MAYEDA, T. K., CLAYTON, R. N. and IKEDA, Y. (1991): Oxygen isotopic studies of carbonaceous chondrite Belgica-7904. Lunar and Planetary Science XXII. Houston, Lunar Planet. Inst., 865–866.
PAUL, R. L. and LIPSCHUTZ, M. E. (1990): Consortium study of labile trace elements in some Antarctic carbonaceous chondrites: Antarctic and non-Antarctic meteorite comparisons. Proc. NIPR Symp. Antarct. Meteorites, **3**, 80–98.
SCORZELLI, R. B. and SOUZA AZEVEDO, I. (1991): Mössbauer spectroscopy studies in Antarctic carbonaceous chondrites Y-86720 and Y-82162. Papers Presented to the 16th Symposium on Antarctic Meteorites, June 5–7, 1991. Tokyo, Natl Inst. Polar Res., 168.
TOMEOKA, K. (1990a): Mineralogy and petrology of Belgica-7904: A new kind of carbonaceous chondrite from Antarctica. Proc. NIPR Symp. Antarct. Meteorites, **3**, 40–54.
TOMEOKA, K. (1990b): Phyllosilicate veins in a CI meteorite: Evidence for aqueous alteration on the parent body. Nature, **345**, 138–140.
TOMEOKA, K. and BUSECK, P. R. (1985): Matrix mineralogy of the Orgueil CI carbonaceous chondrite. Geochim. Cosmochim. Acta, **52**, 1627–1640.
TOMEOKA, K., KOJIMA, H. and YANAI, K. (1989a): Yamato-82162: A new kind of CI carbonaceous chondrite found in Antarctica. Proc. NIPR Symp. Antarct. Meteorites, **2**, 36–54.
TOMEOKA, K., KOJIMA, H. and YANAI, K. (1989b): Yamato-86720: A CM carbonaceous chondrite having experienced extensive aqueous alteration and thermal metamorphism. Proc. NIPR Symp. Antact. Meteorites, **2**, 55–74.

(Received August 16, 1991; Revised manuscript received November 1, 1991)